Current Research in Microbial Sciences 3 (2022) 100139

Contents lists available at ScienceDirect

Current Research in Microbial Sciences

journal homepage: www.sciencedirect.com/journal/current-research-in-microbial-sciences

Histidine kinase two-component response regulators Ssk1, Skn7 and Rim15 differentially control growth, developmental and volatile organic compounds emissions as stress responses in Trichoderma atroviride

Valter Cruz-Magalhães [a,b,1], Maria Fernanda Nieto-Jacobo [a,c,1], Michael Rostás [a,d], Jesus Francisco Echaide-Aquino [a,h], Edgardo Ulises Esquivel-Naranjo [e], Alison Stewart [g], Leandro L. Loguercio [f,*], Artemio Mendoza-Mendoza [a,h,**]

[a] Bio-Protection Research Centre, Lincoln University, Ellesmere Jct Rd, Lincoln 7647, New Zealand
[b] Department of Phytopathology, Federal University of Lavras, Lavras, MG, Brazil
[c] Plant & Food Research Gerald St, Lincoln, New Zealand
[d] Department of Crop Sciences, Agricultural Entomology, University of Göttingen, Wilhelmsplatz 1, Göttingen 37073, Germany
[e] Unit for Basic and Applied Microbiology, School of Natural Sciences, Autonomous University of Queretaro, Queretaro 76140, Mexico
[f] Department of Biological Sciences (DCB), State University of Santa Cruz (UESC), Rod BR 415, Km 16, Ilhéus-BA 45662-900, Brazil
[g] The Foundation for Arable Research, Templeton, New Zealand
[h] Department of Wine, Food and Molecular Biosciences, Lincoln University, Ellesmere Jct Rd, Lincoln 7647, New Zealand

ARTICLE INFO

Keywords:
Biological control
Arabidopsis thaliana
Volatile organic compounds
Environmental stress
Rhizoctonia solani
Sclerotinia sclerotiorum

ABSTRACT

The Skn7, Ssk1 and Rim15 proteins are response regulators involved in osmotic, oxidative and nutritional stress in fungi. In order to verify the involvement of these genes in *Trichoderma atroviride* IMI206040's growth, conidiation, direct antagonism against plant pathogens (*Rhizoctonia solani* and *Sclerotinia sclerotiorum*), production of volatile organic compounds (VOCs) with fungistatic effect, and interaction with plants (growth promotion), single mutants were generated, and the phenotypic patterns were analysed in comparison to the wild-type (*wt*) strain. The mutants were submitted to osmotic, oxidative, membrane and cell wall stress conditions in vitro. The Δ*skn7* and Δ*rim15* mutants did not show either significant differences at morphological level, or marked decreases in mycelial growth and conidiation in relation to *wt*, whereas Δ*ssk1* had altered phenotypes in most conditions tested. The plant-growth promotion of *Arabidopsis thaliana* seedlings induced by VOCs was not quantitatively modified by any of the mutants in relation to the *wt* strain, although possible differences in secondary root hairs was noticed for Δ*rim15*. The fungistatic activity was significantly altered for Δ*ssk1* and Δ*rim15*. Overall, the Δ*ssk1* strain showed remarkable morphological differences, with decrease in mycelial growth and conidiation, being also affected in the antagonistic capacity against plant pathogens. The impacts demonstrated by the deletion of *ssk1* suggest this gene has a relevant participation in the signalling response to different stresses in *T. atroviride* and in the interactive metabolism with phytopathogens and plants. On the other hand, unlike other fungal models, Skn7 did not appear to have a critical participation in the above-mentioned processes; Rim15 seemed to confirm its involvement in modulating cellular responses to nutritional status, although with a possible cross-talk with other cellular processes. Our results suggest that Ssk1 likely plays a key regulatory role, not only in basic metabolisms of *T. atroviride*, but also in biocontrol-related characteristics.

1. Introduction

For a biological organism, 'stress' refers to a departure from conditions that provide optimal growth and survival, usually caused by modifications in the surrounding environment. Microorganisms must be able to perceive environmental stimuli and respond quickly and

* Corresponding authors.
** Corresponding author at: Bio-Protection Research Centre, Lincoln University, Ellesmere Jct Rd, Lincoln 7647, New Zealand.
E-mail addresses: leandro@uesc.br (L.L. Loguercio), artemio.mendoza@lincoln.ac.nz (A. Mendoza-Mendoza).
[1] These authors contributed equally to this work.

https://doi.org/10.1016/j.crmicr.2022.100139
Received 31 December 2021; Received in revised form 2 May 2022; Accepted 16 May 2022
Available online 18 May 2022

adequately to maintain their integrity in a stressing environment (Montibus et al., 2015), causing a metabolic reprogramming for re-adaptation that assures survival in the altered conditions (Leach and Cowen, 2014). As a group of organisms capable of colonizing an extensive array of environments, fungi display a remarkable ecological relevance (Peay et al., 2008). Such a comprehensive adaptive ability depends on the performance of different genetic elements, which induce the synthesis of compounds related to the relief of the stressing condition (Causton et al., 2001). The signalling pathways involved in environmentally induced stress responses in fungi have been extensively studied (Fassler and West, 2011; Chen et al., 2012; Saito and Posas, 2012; Wang et al., 2014; Montibus et al., 2015; Yu et al., 2016), as they also regulate critical cellular processes, such as cell growth, differentiation, sporulation, drug resistance, cell wall biosynthesis, virulence etc. (Oide et al., 2010). Many of the proteins involved in these processes are mitogen-activated kinases (MAPKs), which participate in signalling systems for responses to different types of environmental changes and stresses (Mohanta et al., 2016). Activation of these signalling pathways often occurs through the so-called 'two-component system' (TCS), extensively studied in *Saccharomyces cerevisiae* (Hohmann, 2002).

The TCS is characterized by a sensor and a response regulator. Briefly, the former component is usually a self-phosphorylating protein kinase responsible for sensing the external stimulus, and as a result, donating a phosphoryl group. This group can be transferred directly to another component, the response-regulating protein (RR), or to an intermediate protein responsible for transferring the signal between the sensor and the RR (Posas et al., 1996; Li et al., 1998; Ketela et al., 1998; Santos and Shiozaki, 2001). For the latter component, the signals are transmitted by a 3-step phosphorylation (His-Asp-His-Asp) (Santos and Shiozaki, 2001), including the proteins Sln1 (histidine kinase hybrid), Ypd1 (intermediate protein) and a response regulator protein. The activated RR can directly control the transcription of various specific genes of primary metabolism, or it can transfer the signal to a MAPK that will control (directly or via a signal transduction cascades) the transcription of other stress-related genes (Oide et al., 2010).

Three proteins known as Skn7, Ssk1 and Rim15 are amongst the regulatory elements involved in response to various types of fungal stresses (Oide et al., 2010). The Ssk1 regulator works in response to osmotic and oxidative stresses in *S. cerevisiae* via the MAPK-HOG pathway (Santos and Shiozaki, 2001). It has the signal receiver domain (REC) in its C-terminal portion and has no output domains. The Skn7 regulator has been identified and characterized in studies indicating their participation in the expression of genes necessary for protection against oxidative stress, as the deletion of the *skn7* gene has resulted in increased sensitivity to oxidizing agents (Morgan et al., 1997). Besides the REC domain, this regulator also displays a Heat Shock Factor (HSF) DNA-binding domain in the N-terminal region (Fassler and West, 2011), which can function as a transcriptional activator (Brown et al., 1994). Therefore, this protein operates simultaneously as a sensor and as a response regulator. Its REC–domain activation occurs by a phosphate transference, via the Sln1-Ypd1 phosphorylation pathway, as well as by the Ssk1 (Santos and Shiozaki, 2001). Finally, Rim15 is a RR involved in modulation of the cell cycle in response to nutritional conditions, which is critical for microbial survival (Swinnen et al., 2006). Several cellular functions in fungi are regulated through signalling processes that are dependant upon carbon and nitrogen sources (Liang et al., 2017); this regulator has a prominent role in signalling the cell entry into the G0 phase. Under a condition of nutritional limitation, Rim15 is activated and translocated to the nucleus (Pedruzzi et al., 2003; Urban et al., 2007; Mirisola et al., 2014), where it interacts with transcription factors responsible for activating the expression of stress-response genes (Liang et al., 2017). In this condition, the genes of the ribosome biogenesis are repressed, and as a consequence, genes necessary for the assimilation of alternative sources of carbon and nitrogen are induced (Cutler et al., 2001).

Trichoderma atroviride strains have been used as biocontrol agents for a variety of phytopathogens (El_Komy et al., 2015; Jain et al., 2015; Waghunde et al., 2016) and have contributed to the promotion of growth and relief of several abiotic stresses in plants (Salas-Marina et al., 2015; Lee et al., 2015; 2016; Zeilinger et al., 2016; Medeiros et al., 2017; Zhang et al., 2019; De Palma et al., 2019; dos Santos et al., 2022). This species has been used as an experimental model for several studies, allowing the generation of an array of mutants through consistent and reproducible methods (Hernández-Oñate et al., 2012; Medina-Castellanos et al., 2014; Schmoll et al., 2016). Since the molecular mechanism for signal sensing, transduction and gene expression modulation for Ssk1, Skn7 and Rim15 are different from each other, in this study we reported how wild-type and mutant strains for these three TCS-RR genes from *T. atroviride* behave phenotypically under distinct culture conditions and in vitro treatments. The experimental design aimed at addressing questions related to possible involvement/interference of these genes in both primary and interactive fungal metabolisms with abiotic (nutrition and stress-inducing compounds) and biotic (plants and other fungi) factors.

2. Materials and methods

2.1. Microorganisms and culture conditions

Trichoderma atroviride IMI206040 strain was used as the wild-type (*wt*), and Δ*skn7*, Δ*ssk*1 and Δ*rim*15 single mutants were generated from this strain, based on a strategy previously reported (Hernández-Oñate et al., 2012). Spores of the *wt* and mutant strains were grown in PDA (Difco®) at 25 °C for 7 days, under a 12 h/12 h light/dark regime. This photoperiod was used for all the experiments described below, except when indicated otherwise. The phytopathogen strain of *Rhizoctonia solani* RS73–13b (LU8003) was propagated by applying mycelial discs (5 mm) onto PDA plates. In contrast, a *Sclerotinia sclerotiorum* strain (LU8006) was propagated by the transfer of mature sclerotia to PDA plates. Both were incubated for five days, as described by Steyaert et al. (2016).

2.2. Growth and conidiation under stress conditions

Conidia from the *T. atroviride* strains, grown as described in the previous section, were collected in sterile double-distilled water and filtered through two layers of sterile Miracloth® (Calbiochem™) to eliminate hyphae/mycelia. The collected spores from the *wt*, Δ*skn7*, Δ*ssk*1 and Δ*rim*15 strains were counted in a haemocytometer and adjusted to 10^6 spores in 5 μL water per strain for application on the centre of PDA plates. In addition to the control plates (with no supplement), various distinct stressing conditions (osmotic, oxidative, cell-wall and cell membrane stresses) were tested by supplementing the PDA medium with NaCl (0.5 M), sorbitol (1.0 M), SDS (0.014%), Calcofluor White (CW, 600 μgmL^{-1}), Congo red (CR, 1000 mg/mL^{-1}), or Menadione (0.5 mM). All inoculated PDA plates (treatments and control) were incubated at 25 °C for 7 days (12 h/12 h light/dark). The colonies' diameters were assessed every 24 h during this period, and the total number of conidia produced was also evaluated. Six replicates (plates) per treatment were used, and the whole experiment was repeated three times.

2.3. Direct confrontation assays with T. atroviride wt and mutants

The direct antagonistic assays were performed using the in vitro dual culture method, according to the guidelines described in Steyaert et al. (2016), with some modifications. Mycelial disks (5 mm) of *S. sclerotiorum* or *R. solani* cultures (previously grown in the dark for 5 days in PDA plates; see above), and of the *wt* and mutants from *T. atroviride* were transferred to Petri dishes containing PDA medium and incubated at 25 °C. Growth and mycelial interaction were monitored every 24 h with interaction images being recorded. The evaluation

of the antagonistic treatments was performed when the control plate (without *T. atroviride*) was completely covered by the phytopathogen. The percentage inhibition was calculated by the formula: Inhibition (%) = ([C – T) x 100] / C, in which 'C' = fungal diameter (cm) in the control plate, and *T* = fungal diameter (cm) in *Trichoderma*-treated plates (Steyaert et al., 2016). The experiment was conducted with three replicates for each *T. atroviride* strain (treatment) and were repeated three times.

2.4. Plant-growth promoting effects

The growth-promoting effects of volatile organic compounds (VOCs) synthesized by *T. atroviride* strains upon *Arabidopsis thaliana* was assessed as previously described by Nieto-Jacobo et al. (2017). Five *A. thaliana* (Col-0) seeds per plate were pre-sterilized and then placed on one side of a 90 mm-diameter, two-compartments Petri dish (Labserv™) containing 0.2x MS medium (Murashige and Skoog, Sigma-Aldrich™), supplemented with 0.6% sucrose and pH adjusted to 7.0. Plates were sealed with plastic film and placed on their edge at an angle of approximately 65° (from horizontal level), and incubated at 22 °C under a photoperiod of 16 h light / 8 h dark. After 7 days of culture, a 5 ul suspension containing 10^6 *Trichoderma* spores was applied into the opposite compartment from the seedlings. The plates were re-sealed and incubated for an additional 7 days. Fresh weight of shoot, roots and total biomass (roots + shoot) per plant were measured. Forty plants per treatment (8 plates) were used, and the assays were repeated three times.

2.5. Fungistatic effects of T. atroviride VOCs

The impact of *T. atroviride* VOCs from *wt*, Δ*skn*7, Δ*ssk*1 and Δ*rim*15 on *R. solani* and *S. sclerotiorum* growth was determined using the method described by Steyaert et al. (2016). A 5 mm-diameter disc of *Trichoderma* mycelium (3-days culture) was applied onto Petri dishes (90 × 25 mm) containing PDA medium and incubated for 48 h at 25 °C. Two days after inoculation of *Trichoderma*, additional PDA plates were inoculated with a 5-mm mycelial disc from a colony of *R. solani* or from *S. sclerotiorum*, previously cultured for 72 h, as described above. The lids of the plates with *Trichoderma* were replaced by the plates inoculated with the phytopathogens, so that the fungi were facing each other, in a single-chamber system. Both plates were sealed together with a triple layer of plastic film to prevent loss of the volatile compounds. The phytopathogenic fungi were set on top to avoid potential contamination by *Trichoderma* conidia. PDA plates containing only the phytopathogens were used as controls. All these single-chamber dual plates were incubated under the same conditions as indicated above. The diameter of the phytopathogen growth was recorded every 24 h. After 7 days, the fungistatic activity of VOCs from *T. atroviride wt* and mutants was stopped by removing the plates containing *Trichoderma* and replacing them back with the sterile lids, thus allowing the *R. solani* or *S. sclerotiorum* fungi to resume their growth for additional 7 days under the same incubation conditions. Five plates were used per treatment, and the assays were repeated three times.

2.6. Analysis of VOCs profiles by T. atroviride wt and mutants

The profiles of VOCs produced by *T. atroviride* strains were performed as previously described by Nieto-Jacobo et al. (2017), which were based on gas chromatography coupled to Shimadzu GCMS-QP2010 mass spectrometer (Shimadzu™ Co., Japan), and equipped with a Restek Rxi-5 ms fused silica capillary column (30.0 m x 0.25 mm id x 0.25 μm, Bellefonte, PA, USA).

2.7. Carbon and nitrogen usage profiles of T. atroviride wt and mutants

The study on usage profiles of different C and N sources was done by using the Biolog FF MicroPlate™ and Biolog PM3B MicroPlate™ systems (Biolog Inc., Hayward, CA, USA). The experiments were conducted as described by Friedl et al. (2008) with some modifications. *Trichoderma* conidia were suspended in sterile inoculating fluid supplied along with the Biolog Plates kits and vortexed; the spores concentration were adjusted to an absorbence reading (optical density, OD) of 0.2 at 600 nm and the conidial suspensions (100 μL per testing strain) were distributed into the wells; the plates were incubated at 25 °C, under a 12 h/12 h light/dark regime. ODs related to mycelial growth (at 750 nm) and mitochondrial activity (at 490 nm) were assessed at 0 h, 24 h, 48 h, 96 h and 120 h, using a microplate reader (Multiskan GO, Thermofisher Scientific™). The values referring to OD at 750 nm at 120 h were used as reference points for analysis of the mycelial growth, as they allowed better comparison of the biomass formation in all carbon and nitrogen sources. The experiments were done in independent triplicates. To quantify the conidia, a previously defined scale based on scores (Friedl et al., 2008) was used as follows: '0′ = total absence of conidia and conidiophores, '1′ = formation of immature pustules without mature conidia, '2′ to '5′ = four levels of conidiation, ranging from weak and diffuse conidia (2) to total conidia development and coverage of the entire well (5). These levels were defined by visual inspection with further aid of a colony counter. The mean values per time point were used for statistical analyses. A clustering procedure of C and N sources per strain was performed by using Euclidean distance of the mean values at each time. This method was used to analyse both types of nutritional sources, according to the growth and conidia profile presented by the strains.

2.8. Statistical analyses

Data from all experiments, except Biolog Phenotype Microarrays™, were subjected to analysis of variance (ANOVA) separately and the means were compared by the Tukey's test ($p < 0.05$) using the *TukeyC* package (Faria et al., 2018) in the 'R' platform (Team, 2013). To analyse the mycelial growth and conidiation data generated by the Biolog Phenotype Microarrays™ system, we used multivariate analysis for data clustering and generated heatmaps using the *gplot* package (Warnes et al., 2016) from the R platform.

3. Results

3.1. Ssk1 is longer than predicted

Conserved domains present in the amino acid sequences of the three stress-response regulatory proteins were identified in *T. atroviride* IMI206040 (Fig. 1A). The amino acid sequence of Ssk1 showed only the response regulator (RR) domain of the REC type, a receptor domain homologous to the CheY (Hess et al., 1988). For Skn7, its amino acid sequence showed a binding domain that is homologous to HSF (Heat Shock Factor) and specific to certain DNA sequences (Sorger, 1991), in addition to the REC domain. The Rim15 amino acid sequence, on its turn, showed four identifiable domains: PAS (Per-Arnt-Sim), PK (Protein Kinase), AGC kinase and a RR domain of the REC type, as predicted in *S. cerevisiae* (Swinnen et al., 2006). Alignment of the RR domains from Ssk1, Skn7 and Rim15 showed the conservation of key amino acids for these stress-response regulators in *T. atroviride* (Fig. 1B); a putative phosphorylation site was found (indicated by an asterisk), which corresponds to an amino acid that works as receptor of phosphate groups. The number of predicted amino acids for the Rim15, Skn7 and Ssk1 RRs in *T. atroviride* was 1944, 581 and 1233, respectively (Fig. 1A). Interestingly, the Ssk1 protein in *T. atroviride* is longer than initially predicted when compared to its homologous (Fig. 1A and 1C), e.g., in *S. cerevisiae* (721aa) (https://www.yeastgenome.org/locus/S000003996). As shown in Fig. 1D, this larger size for *T. atroviride* Ssk1 was confirmed after alignment with a series of sequences for this protein characterized from various species of *Trichoderma*.

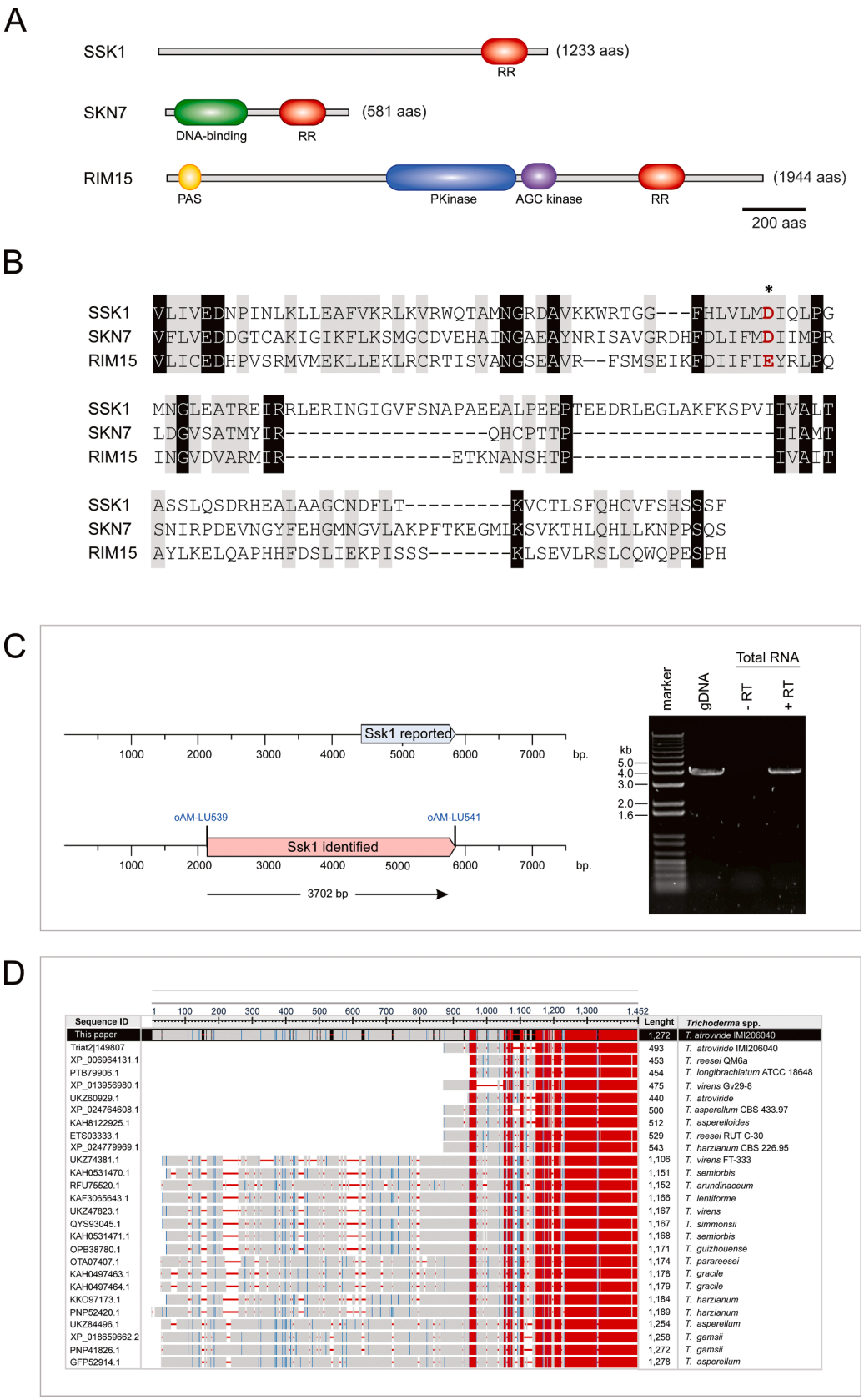

Fig. 1. Structure and sequence of the histidine kinase response regulators Ssk1, Rim15 and Skn7 from *T. atroviride* IMI206040 strain. **(A)** Domain structure of Ssk1, Rim15 and Skn7. The protein domains were identified in InterPro (https://www.ebi.ac.uk/interpro/); the receiver domains are indicated as RR (red circles). **(B)** ClustalW-based sequence alignment between the receiver domain of Ssk1, Rim15 and Skn7 from *T. atroviride*. Ssk1 (JGI Protein ID: 149,807); Rim15 (JGI Protein ID: 320,942) and Skn7 (JGI Protein ID: 137,669) sequences were obtained from JGI (https://mycocosm.jgi.doe.gov/Triat2/Triat2.home.html). Dashed lines represent gaps in the alignment. Conserved amino acid residues between the three proteins are indicated in black, and the semi conserved residues in grey. The conserved aspartic acid from Ssk1 and Skn7 are indicated in red, while in Rim15, a glutamic acid in the same position has been observed in other orthologues in fungi. **(C)** Schematic view of the predicted 1400-bp *ssk1* (ID: 149,807) by JGI ('Ssk1 reported' region), compared to a 3702-bp intron-less open-reading frame (*orf*) identified for *ssk1* ('Ssk1 identified' region) after PCR amplification of genomic DNA, using oAM-LU539 (5′-TTACATATGGCGCCTGACATTGCTAA-3′) and oAM-LU541 (5′-TAAGGATCCGTTTGTACTTTTGTCTGGTGAGACA-3;') primer-pair. To confirm this suggested larger *orf*, a *ssk1*-derived cDNA was created using total RNA isolated from *T. atroviride* IMI206040 mycelia grown on PDB medium for 72 h; as shown in the gel, those primers were used in PCR amplification without (–RT) or with reverse transcriptase (+RT), to amplify a ~4k-bp fragment. **(D)** Alignment of publicly available Ssk1 orthologues from other *Trichoderma* species. The first line represents the larger *orf* identified in this work.

3.2. Influences of Ssk1, Skn7 and Rim15 response regulators (RR) in growth and conidiation of T. atroviride

To study the phenotypic effects for the loss-of-function of these three RRs in *T. atroviride*, single mutants for the genes *ssk1* (JGI Protein ID: 149,807), *skn7* (JGI Protein ID:137,669) and *rim15* (JGI Protein ID: 320,942) were generated (Supplementary methods). The effects on growth and conidiation of the *wt, Δssk1, Δskn7* and *Δrim15* strains were assessed under conditions of osmotic (0.5 M NaCl or 1.0 M sorbitol), oxidative (0.5 mM Menadione), cell wall (600 μg mL^{-1} Calcofluor white or 1000 mg mL^{-1} Congo Red) or membrane (0.014% SDS) stress. With the exception of the osmotic stress, the *Δskn7* and *Δrim15* mutants showed a similar morphological pattern to each other and to *wt* for all the conditions tested, whereas the *Δssk1* presented visibly distinct morphologies (Fig. 2A). On the other hand, under the specific conditions of osmotic stress (NaCl and Sorbitol), all mutants presented altered phenotypes in relation to *wt*. In this condition, *Δrim15* and *Δskn7* presented a lower colony size than the *wt*, whereas *Δssk1* was severely affected, showing no sign of mycelial growth (Fig. 2A and 2B). The stress condition caused by Menadione (oxidative stress) caused a significantly higher relative growth for *Δssk1* than for *Δrim15*, although they were not different to *wt* and *Δskn7* (Fig. 2B). In the plasma-membrane stress condition (SDS), only *Δssk1* showed significantly less mycelial growth than the *wt; Δskn7* showed significantly higher growth than other mutants but not than *wt* (Fig. 2B). The observed alteration in colony colour for *Δssk1* in SDS (Fig. 2A) was probably related to the observed reduction in conidia production (Fig. 2C). This strain was also the only one with mycelial growth affected under cell-wall stress conditions (CW and CR) (Fig. 2A and 2B).

Overall, it is noteworthy that no conidia were produced for any strain under conditions of osmotic stress (NaCl and Sorbitol), and that *Δssk1* underwent a significant reduction in conidiation for all stress treatments tested, as well as for the PDA-only control (Fig. 2C). For the *Δrim15* and *Δskn7* mutants, their conidiation values were statistically similar to those of *wt* except for the CW stress, in which the conidiation values for all strains were significantly different from each other, following the descending order of *Δrim15* > *wt* > *Δskn7* > *Δssk1* (Fig. 2C). The conidiation for the *Δskn7* mutant was significantly lower than *wt* only for the PDA control and higher only for the cell-membrane SDS stressor (Fig. 2C). The *Δrim15* behaved mostly as the *wt* for all treatments.

Additionally, we evaluated the effect of light on the growth of *wt, Δssk1, Δskn7* and *Δrim15* strains under conditions of oxidative (Menadione and H_2O_2) and cell wall (Congo Red) stresses. Most of the growth patterns observed in such assays were in agreement with the expected effects shown in Fig. 2. In general, all strains tested exhibited lower mycelial growth under the light condition (Supplementary Fig. S1). This is expected, since the light condition is an oxidative-type of abiotic stress factor, which has a direct impact on the regulation of DNA repair systems. Interestingly, *Δrim15* was more severely affected in 40 mM H_2O_2 stress treatment in the dark, showing a lower colony size than the *wt* and the other strains (Suppl. Fig. S1).

3.3. Nutrients assimilation in the Δssk1, Δskn7 and Δrim15 mutants

The profiles of carbon and nitrogen sources assimilation were assessed for growth and conidiation of all strains (Suppl. Fig. S2). A considerably higher variation in the patterns of assimilation was observed for mycelial growth than for conidiation, in both types of nutrients tested. Considering the entire nutrients-consumption profiles, C sources were generally more discriminative of individual *T. atroviride* strains than N sources; in this sense, while only 15 and 6 single C sources did not show differences in growth and conidiation, respectively, for all tested strains (Suppl. Fig. S2A and 2C), 20 and 22 individual N sources could not discriminate the strains in growth and conidiation, respectively (Suppl. Figs. S2B and S2D). A goodness-of-fit chi-square analysis rejected the null hypothesis of an equal number of individual C and N sources as being incapable of discriminating the four strains ($p = 0.021$). Due to this more discriminative power of C sources, a more evident grouping of the strains was observed: two groups were formed for mycelial growth (*wt* + *Δssk1* and *Δskn7* + *Δrim15*) and a group with remarkable similarities amongst their three members (*wt* + *Δssk1* + *Δskn7*) for conidiation (Fig. 2A and 2C). N sources were much less discriminative of strains for mycelial growth but more discriminative in terms of conidiation results (Supplementary Fig. S2B and 2D). Interestingly, based on the C and N assimilation profiles, the *Δrim15* appeared to have been more strongly affected in terms of conidiation than in mycelial growth when compared to *wt* and the other mutants (Suppl. Fig. S2C and 2D). As discussed further below, these patterns are consistent with a role of Rim15 in the regulation of metabolisms related to nutrients assimilation in fungi.

3.4. Influence of Ssk1, Skn7 and Rim15 RRs in the direct interaction of T. atroviride with other fungi

To verify whether the RRs under study interfere in the fungus-fungus interactive phenotypes, direct confrontation assays between the *T. atroviride wt* and mutant strains against *Rhizoctonia solani* and *Sclerotinia sclerotiorum* plant pathogens were assessed. The results for *R. solani* showed three distinct morphological patterns of growth/interaction: one represented by the *wt* and the *Δskn7* mutant, another by the *Δrim15* and the last by the *Δssk1*, although the inhibition of *R. solani* was not significantly different between the latter two (Fig. 3). The quantitative levels of growth inhibition observed for this phytopathogen confirmed the existence of the indicated morphological patterns (Fig. 3). On the other hand, the challenges against *S. sclerotiorum* showed an overall different morphological phenotype of inhibition, but a similar grouping pattern for the strains under study, i.e., *Δskn7* morphology was more similar to that of *wt*, whereas *Δrim15* was closer to *Δssk1*; however, these two inhibition groups were not confirmed quantitatively, as only *Δssk1* was significantly less inhibitory than the *wt* (Fig. 3). In general, when comparing the results for both pathogens, the *T. atroviride* strains appeared to have a stronger antagonistic capacity against *R. solani*, whereas *S. sclerotiorum*, on the other hand, appeared to have a greater competition and resistance ability against the *Trichoderma* strains of this study (Fig. 3). For both pathogens, the inhibition phenotypes of the *Δssk1* mutant was the most affected one, followed by those of *Δrim15*; the least effect for the loss of function was observed for *Δskn7* in relation to *wt* (Fig. 3).

3.5. Influence of the three stress RR in the production of volatile organic compounds (VOCs) with effects on growth and morphology of Arabidopsis thaliana seedlings

The production and emission of volatile organic compounds (VOCs) by fungi is known as a 'wireless' type of communication between plants and microbes in nature (Bitas et al., 2013; Schmidt et al., 2015). To assess the influence of the three fungal RRs under study in the growth and morphology of plantlets, sealed-chamber experiments were performed with *Arabidopsis thaliana* seedlings and the *wt* and mutant *T. atroviride* strains. All the tested strains led to a significant increase in partial and total biomass of *A. thaliana* seedlings when compared to control plants (Supplementary Fig. S3). Interestingly, a particular phenotype was noticed for the *Δrim15* treatment: in terms of the VOCs' effects of the *T. atroviride* strains on plant growth promotion, there were no significant differences in the biomass values between the *wt* and mutant treatments; nevertheless, the *Δrim15* mutant's volatiles led to a specific morphological structure of *A. thaliana* roots, which visibly presented more lateral roots compared to the control and the other mutant treatments (Suppl. Fig. S3). Furthermore, the remarkable changes observed in growth and developmental morphology observed for the *Δssk1* strain did not apparently alter its ability of synthesizing/emitting VOCs with plant growth-promotion capacity (Suppl.

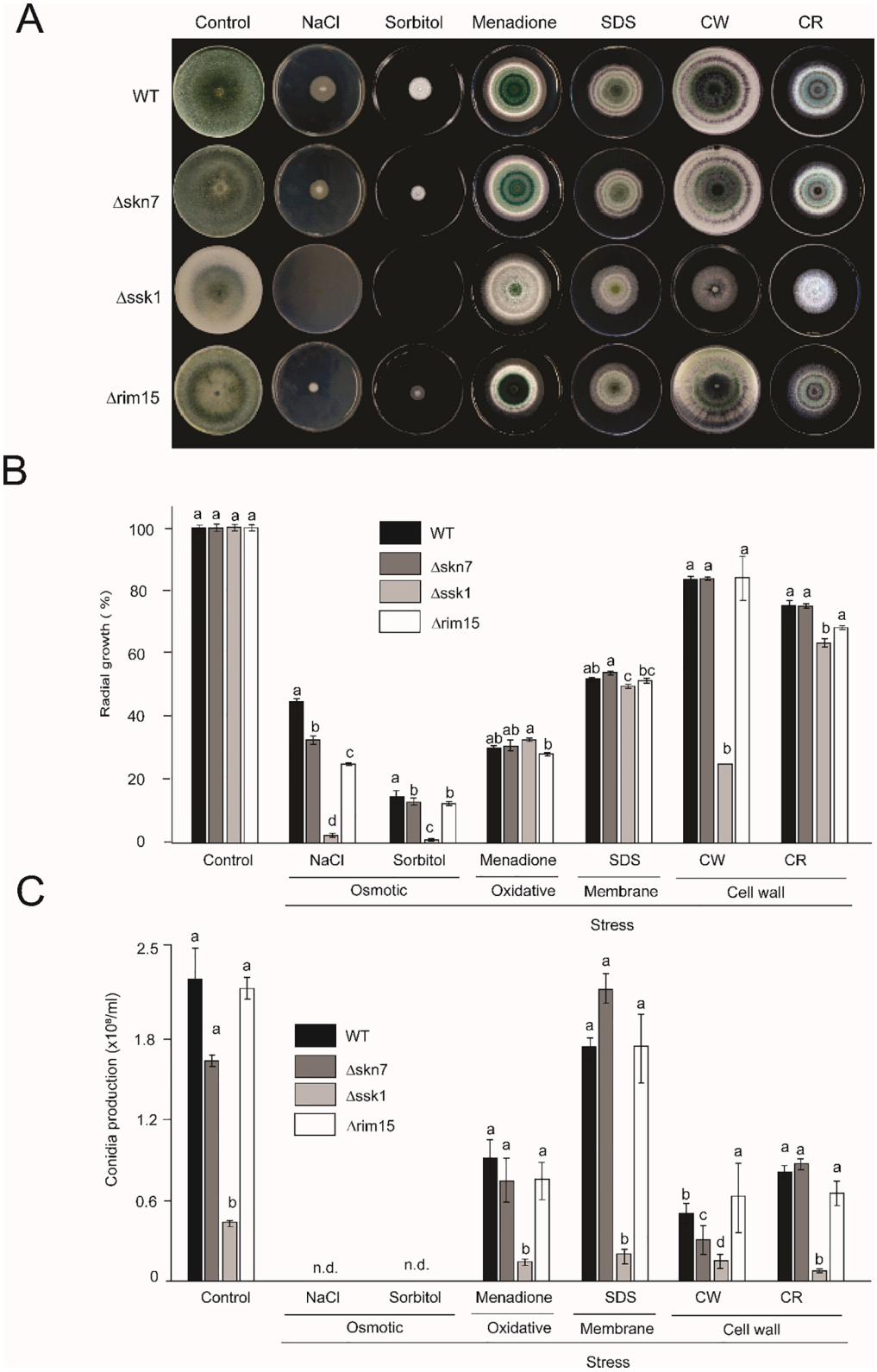

Fig. 2. Patterns of morphology, growth and conidiation of Δ*skn*7, Δ*ssk*1, and Δ*rim*15 strains, compared to the *wild-type* (*wt*) of *Trichoderma atroviride* IMI206040, subjected to culture medium supplemented with distinct stressing agents. (**A**) Morphological patterns presented by the *T. atroviride* strains under different stress conditions. (**B**) Relative values of mycelial growth. Plotted mean values and error bars come from six replicates for each of the treatments, which were evaluated in relation to the reference control data (100%). (**C**) Conidia quantification. Plotted mean values and errors were obtained from 3 plates per treatment. The experiments were repeated three times with similar results. Analysis of variance was performed, and the means were compared by the Tukey's test ($p < 0,05$). Different letters on top of bars indicate statistically significant differences amongst strains within each treatment of stressing agent. SDS, Sodium dodecyl sulphate; CW, Calcofluor White; CR, Congo Red.

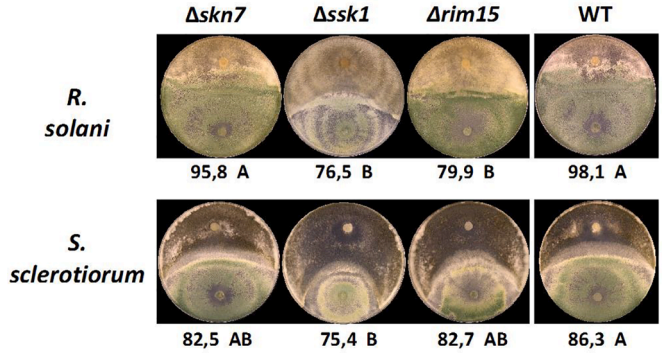

Fig. 3. Comparison of direct antagonism of *Trichoderma wt* and RR mutant strains against *R. solani* and *S. sclerotiorum*. The *wt*, Δ*skn7*, Δ*ssk*1 and Δ*rim*15 strains appear at the bottom half of the dual-culture plates, whereas the phytopathogens (indicated on the left) appear in the top half. The values below each plate represent the mean inhibition rates calculated from three biological replicates. The different letters within the plate series of each pathogen indicate significant differences by Tukey's test ($p < 0.05$).

Fig. S3).

3.6. Effects of RRs in the production of T. atroviride VOCs with fungistatic action

Since *Trichoderma* spp. have been reported as capable of producing volatile compounds with fungistatic action against other fungi (Kottb et al., 2015; Cruz-Magalhães et al., 2019), we evaluated such an ability of the *T. atroviride* strains under study in a single-chamber system (paired plates) against *R. solani* and *S. sclerotiorum* (Fig. 4). All strains produced VOCs with significant inhibitory effects on the growth of both pathogens tested, which were able to resume growth after removing the *Trichoderma wt* and RR mutants (Fig. 4). However, although these patterns were overall similar for both pathogenic fungi, the activity of those VOCs appeared to be pathogen-specific. While the *wt* and *Δskn7* showed a stronger and significantly different inhibition of *R. solani* than did *Δssk1* and *Δrim15*, such differences amongst strains were less pronounced for *S. sclerotiorum* (Fig. 4), consistent with the higher resistance shown by this pathogen to the *Trichoderma* strains in the direct confrontation assays (Fig. 3). Based on the results for both pathogens, the loss of function for the *ssk1* gene showed a significant decrease in the fungistatic VOCs emission when compared to *wt*, whereas no significantly different phenotypic effect was observed for the *skn7* (Fig. 4); for the *Δrim15* strain, the effect observed was pathogen-specific, being different than *wt* only for *R. solani* (Fig. 4A and 4B).

3.7. Profile of volatiles emitted by the T. atroviride wt and mutants strains

Considering that the VOCs produced by all the *T. atroviride* strains under study had a fungistatic effect against *R. solani* and *S. sclerotiorum* phytopathogens (Fig. 4), but that they did not show any significant difference in their effects on growth and biomass of *A. thaliana* (Suppl. Fig. 3), we assessed the general profile of these compounds produced by the four strains, using a micro phase extraction system followed by GC–MS determination. As it could be seen from Table 1, in relation to the *wt*, each mutation caused an effect not only on the total amount of VOCs produced, but also in the relative proportion of various compounds within the set of volatiles produced. An interesting observation was that the total amount of volatiles detected per strain did not appear to correlate with fungistasis, as the Δ*ssk1* and Δ*rim15* showed the highest amounts of total VOCs (Table 1), but the lowest inhibitory

Table 1
Percentages of total VOCs production from *Trichoderma atroviride* (IMI206040) wild type, Δ*skn7*, Δ*ssk1*, and Δ*rim15* strains.

Class	Compounds[1]	*T. atroviride* IMI206040			
		Wild type	Δ*skn7*	Δ*ssk1*	Δ*rim15*
–	Total VOCs detected (RPA) [2]	106.02	51.24 (%) [3]	146.18	313.49
OT-1	2-Methyl-1-butanol	1.8	10.2	2.4	2.9
C7–1	2-Heptanone *	40.3	51.0	9.7	5.3
C7–2	2-Heptanol *	3.9	6.3	1.2	0.4
C8–1	1-Octen-3-ol	0.28	1.0	0.7	0.0
C8–2	3-Octanone	2.2	10.3	10.8	0.3
C9–1	2-Nonanone *	1.8	5.3	0.3	0.3
FU-1	2-Pentyl-furan	1.0	3.0	2.5	4.6
MT-1	p-Menth-2-en-7-ol	0.2	0.7	0.2	0.1
ST-1	α–Bergamotene	0.1	0.1	0.05	2.0
6PP-1	6-Pentyl-2H-pyran-2-one	35.7	0.6	65.7	46.4
6PP-2	(E)−6-Pent-1-enylpyran-2-one	0.9	0.0	1.4	1.1
–	*Others*	*11.8*	*13.8*	*5.1*	*36.6*

[1] Volatile Organic Compounds were measured by gas chromatography coupled to a mass spectrometer (GC–M–). This Table summarizes some of the values presented on Supplementary Table S1, aiming at illustrating most relevant VOCs for the scope of this study.

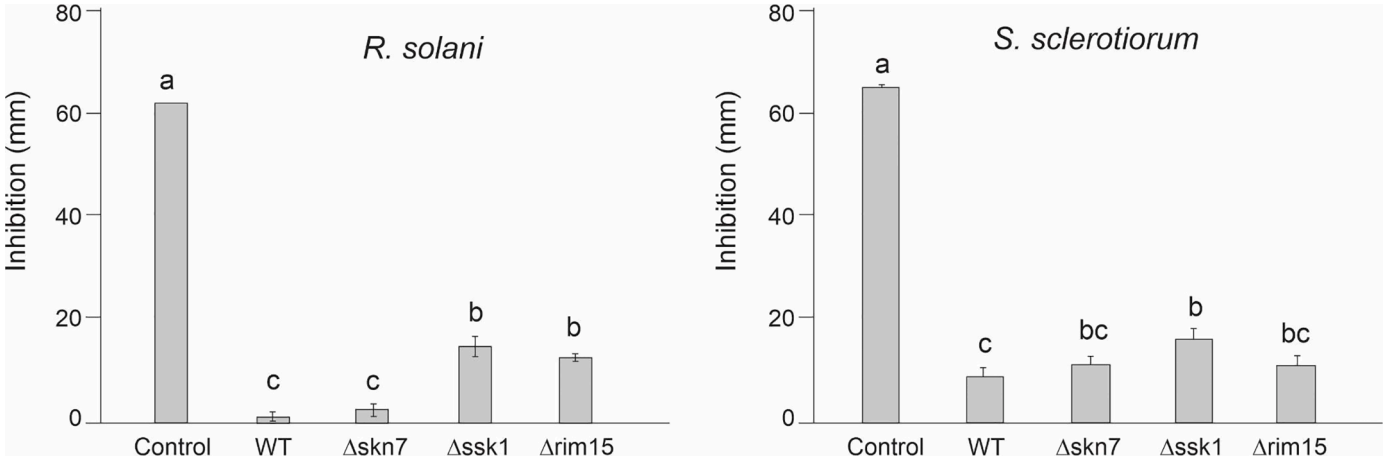

Fig. 4. Fungistatic activity of VOCs from *T. atroviride wt* and RR mutants against two phytopathogens in sealed, paired-plates system. The inhibition effects of VOCs produced by the *Trichoderma* strains were evaluated by gauging mycelial growth of (**A**) *R. solani* and (**B**) *S. sclerotiorum*. This growth (in mm) was an average of 4 replicates, being subjected to Analysis of Variance (ANOVA). Different letters at the top of the bars indicate statistical differences by the Tukey's test ($P < 0.05$). The experiment was performed twice with similar results.

effects on the pathogens (Fig. 4). Therefore, the fungistatic effects observed were likely a result of the specific activity of one or a few volatiles within the whole set, or yet, the result of a particular combination of them. An array of 29 volatile compounds produced by the *wt* strain were detected (Suppl. Table S1); however, only two of them, 2-Heptanone (C7–1) and 6-Pentyl-2H-pyran-2-one (6PP-1), comprised 76% of all VOCs. Despite these two compounds were also highly represented within the sets of mutants' VOCs (51.5% of Δ*skn*7, 75.4% of Δ*ssk*1 and 51.7% of Δ*rim*15, Table 1), only *wt* was able to produce high percentages of both compounds simultaneously. The Δ*skn*7 showed a dramatic decrease of 6PP-1, whereas the other two mutants proportionally increased it in relation to *wt*. On the other hand, Δ*ssk*1 and Δ*rim*15 sharply reduced the amount of 2-heptanone, whereas Δ*skn*7 increased it (Table 1). A detailed inspection on the proportion (Table 1) and absolute values (Supplementary Table S1) of the specific VOCs produced by the *wt* and mutants revealed that the patterns of variation found for 2-Heptanone, 2-Heptanol and 2-Nonanone agree with the fungistatic effects observed for the *T. atroviride* strains (Figs. 3 and 4). Interestingly, despite being the mutant with remarkably less total amount of VOCs produced, Δ*skn*7 produced proportionally higher levels of those three volatiles, and yet, was as fungistatic as the *wt* (Fig. 4).

4. Discussion

Trichoderma spp. are cosmopolitan filamentous fungi, found in several environments and widely used in agriculture as the basis of various bioproducts, the majority of which related to biological control (Druzhinina et al., 2011; Hermosa et al., 2012; Szczalba et al., 2019; Adnan et al., 2019). In this context, *T. atroviride* is one of the most used biocontrol-agent species, having a recognized action also in the relief of abiotic and biotic stresses, promotion of plant growth, direct physical antagonism against other fungi, and induction of plant resistance to phytopathogens (Zeilinger et al., 2016; Druzhinina et al., 2011; Hermosa et al., 2012; dos Santos et al., 2022). These features result from a complex metabolic network involving a series of response regulator (RR) proteins. The interaction of a given strain genotype with environmental conditions (i.e. nutrient availability, pH, moisture, temperature, etc.) defines the outcomes of these characteristics (Nieto-Jacobo et al., 2017). In this study, we used loss-of-function single-mutants of *T. atroviride* to address the effects of three stress-related RRs, namely Skn7 (oxidative), Ssk1 (osmotic) and Rim15 (nutrition). Their possible implications on growth and reproduction (primary metabolisms) of *T. atroviride*, as well as on its interaction with plants and other fungi are discussed.

Considering qualitative (morphology) and quantitative (growth and conidiation) phenotypes, the comparative analysis of the *T. atroviride wt* and mutants suggests that the three RR genes somewhat modulate the fungal response to different stresses, although the lack of function for Skn7 and Rim15 appeared to have a much lower impact on the fungus metabolism/physiology than Ssk1 (Fig. 2). The significantly altered morphology, growth and conidiation observed for *Δssk1* colonies for virtually all stress conditions tested likely indicates a general role of Ssk1 in stress-response regulation in *T. atroviride*, similarly to what has been described in the *Candida albicans* (Chauhan et al., 2003) and *Alternaria alternata* (Yu et al., 2016) models. In addition, the total lack of growth of *Δssk1* under the osmotic stress conditions given by NaCl and Sorbitol (Fig. 2) strongly suggests a direct regulatory role for Ssk1 in this particular type of stress, as previously reported in other fungal models (Horie et al., 2008; Chen et al., 2017; Liu et al., 2017; Rodriguez-Gonzalez et al., 2017). Finally, under the cell wall stress conditions (CW and CR treatments), *Δssk1* was the only strain that showed a significant reduction in mycelial growth. Taken together, these results not only suggest the possibility of a crosstalk between the oxidative, osmotic and nutritional stress responses signalling pathways in *T. atroviride* (Friedl et al., 2008), but they also point to an upstream regulatory action of Ssk1, in relation to Skn7 and Rim15, in modulating these response metabolisms. Interestingly, despite the observed reduction in mycelial growth under the oxidative stress generated by Menadione, *Δssk1* was able to grow significantly more than the other strains (Fig. 2B), which suggests that *ssk*1 expression in *wt* may exert a repressive (or negative) mode of growth regulation under this stress condition.

Congo red (CR) and calcofluor white (CW) are two fluorophores that act as stressing agents (Roncero and Duran, 1985; Nodet et al., 1990), due to binding to polysaccharides, explicitly affecting the glucan (CR) and chitin (CW) chains, thereby compromising the integrity of the cell wall. Considering a similar culture time, the *wt* and mutant strains grew less in CR than in CW (Fig. 2A and 2B), suggesting that *T. atroviride* seems more sensitive to disruption of the glucan chains in the assembly of its cell wall. However, the loss-of-function for Ssk1 was apparently of a larger magnitude for the CW stress (Fig. 2B), thus suggesting a more intense regulatory role on maintenance of the chitin chains integrity. Since no strain was able to conidiate when cultured in medium supplemented with osmotic stress agents (NaCl and Sorbitol, Fig. 2), a minimally proper osmolarity appears to be essential for the conidiation process in *T. atroviride*. For the plasma membrane stress condition caused by SDS, the *Δskn7* strain was able to produce more conidia than the others (Fig. 2), which possibly indicate the involvement of Skn7 as a negative regulator of conidiation in *T. atroviride*.

Since light is a well-acknowledged factor that affect growth and conidiation in *Trichoderma* (Casas-Flores et al., 2004; Steyaert et al., 2010), we have also evaluated its effects on mycelial growth of the four *T. atroviride* strains under study, in combination with oxidative and cell wall stresses. Indeed, light affected the growth of *T. atroviride*, since all strains tested showed a reduced-growth phenotype (Supplementary Fig. S1). This is not unexpected, as the MAPK Tmk3 pathway has already been shown to be essential for *T. atroviride* in the regulation of DNA repair systems operating in the dark (Esquivel-Naranjo et al., 2016). Interestingly, since the participation of Rim15 was expected in the response metabolism to nutritional stress, it was surprising that Δ*rim*15 was affected in the condition of oxidative stress (H_2O_2 40 mM) in the dark (Suppl. Fig. S1A and 1B).

The profiles of carbon and nitrogen sources assimilation by the *T. atroviride* strains revealed a more relevant variation in their effects on mycelial growth than on conidiation (Suppl. Fig. S2). This suggests that the three RR genes are likely involved in a greater variety of biochemical pathways related to vegetative growth than to reproductive processes, when considering either positive or negative regulatory modes. Rim15 has been reported as a RR for nutritional stress (Inai et al., 2013) such that the loss of its function should expectedly lead to difficulties in metabolizing C and N sources, and so, cause an overall lower growth and conidiation. Indeed, considering the general nutrients-consumption profiles, this condition showed to be truer for conidiation than for mycelial growth and for C than for N sources; for mycelial growth, though, *Δrim15* was as much different from *wt* as were the other mutants (Suppl. Fig. S2). These results would suggest a more critical involvement of Rim15 in regulation of reproductive metabolisms, likely with a positive mode of action, as the loss of its function tended to decrease conidiation. We also suggest that, in terms of conidiation, carbon-sources metabolisms would be more subjected to regulation by Rim15, since a greater impact of different C sources was perceptible when compared to the N nutrients (Suppl. Fig. S2C and 2D, respectively). The results also indicated that a number of C and N nutrients seem not usable by *T. atroviride* either for growth or conidiation metabolisms. For the other sub-sets of C and N nutrient sources in which mutants grew and/or sporulated more than *wt*, the respective RR genes likely function in repressive (or negative) regulatory modes (Suppl. Fig. S2). To shed further light on specific metabolisms in which the three RR proteins might be involved, additional studies are currently in progress to evaluate specifically affected/altered biochemical pathways, based on the patterns of growth and conidiation observed for each nutrient, in each *T. atroviride* strain (to be published elsewhere).

Based on what was observed for the direct antagonism against *R. solani*, Δ*skn*7 did not appear to have been affected in this ability

(Fig. 3), which suggests that Skn7 may not be directly involved in metabolic pathways related to such trait. The opposite seems to be true for both Δ*rim15* and Δ*ssk1*, in which a significantly stronger phenotypic effect was observed for the latter, for both pathogens (Fig. 3). Taking into account an overall decrease for growth and conidiation displayed by the Δ*ssk1* (Fig. 2), the idea of a broad involvement of Ssk1 in regulating a variety of relevant metabolisms / biochemical pathways can be advanced. Hence, an affected fungal development resulting from this RR loss of function may be the primary cause of the decreased antagonistic activity observed (Fig. 3). Nevertheless, this possibility does not rule out a possible direct involvement of Ssk1 in cellular processes related to fungus-fungus hyphal interaction responses. Concerning the activity of Rim15 in *T. atroviride*, it may be interesting to speculate about how this RR could be related to the decrease in direct antagonistic activity observed (Fig. 3), since the Biolog™ plates resulting profiles for Δ*rim15* (Suppl. Fig. S2) and other previous studies (Swinnen et al., 2006; Liang et al., 2017) have related Rim15 with nutritional stress responses. The most logical inference would be that the observed pattern of a reduced competitive potential of Δ*rim15* with both phytopathogens (Fig. 3) may be related to a possibly reduced ability in regulating nutrients uptake/metabolism caused by the loss of Rim15 function. In general, despite that these in vitro assays are not enough to predict efficiency/efficacy of antagonistic behaviour in the field (Utkhede and Sholberg, 1986; Loguercio et al., 2009), the distinct results from *Trichoderma* vs *R. solani* and vs *S. sclerotiorum* confrontation assays reinforce a common view that microbial antagonistic interactions are strain/species-specific.

Microbial VOCs work as a complex communication/signalling 'wireless' network involving microorganisms and plants (Schmidt et al., 2015). The production of VOCs by fungi has been receiving special attention with regards to their ecological roles in nature (Bitas et al., 2013; D'Alessandro et al., 2014). Previous studies have shown that VOCs from *Trichoderma* strains can promote the growth of *A. thaliana* trough VOCs (Hung et al., 2013; Lee et al., 2014; 2015; Jalali et al., 2017; Nieto-Jacobo et al., 2017; Cruz-Magalhães et al., 2019), a trend confirmed by our results. Although the RR mutants were not different from *wt* in terms of biomass accumulation effects on the seedlings (Suppl. Fig. S3), the VOCs from the *T. atroviride* mutant strains (specially *Δrim15*) seemed to have affected the architecture of *A. thaliana* roots, agreeing with previous studies done in a fungus-plant co-culturing scheme (Nieto-Jacobo et al., 2017). The results pointed towards possible qualitative effects of Rim15 and Ssk1 in the root system architecture, with a likely repressive/negative regulatory action on the development of *A. thaliana* lateral roots (Suppl. Fig. S3). We also cannot rule out a possible indirect involvement of *ssk1*, as a result of an overall lower growth of the corresponding mutant strain, which might have affected the synthesis of plant-interacting VOCs (Suppl. Fig. S3). Experiments in which one varies the amount of initial *Trichoderma* conidia and the exposure times can provide a further in-depth assessment of these issues.

The blend of microbial VOCs that induce plant-growth promotion can also contain specific compounds with fungistatic effects at a distance against other microorganisms (Lee et al., 2016; Jalali et al., 2017). Our results confirmed these phenotypes, suggesting that the RRs under study are not critical for the fungistatic VOCs synthesis, but their loss of function can alter/reduce the fungistasis effects, in a pathogen-specific mode (Fig. 4). The significant decrease in the fungistasis effect observed for *Δssk1,* for both pathogens (Fig. 4), strengthens even further the possibility raised by a comprehensive assessment of the previous experiments; taken together, all the results suggest that Ssk1 appears to be more broadly involved in an array of responsive metabolisms, as the various assessed phenotypes of its *T. atroviride* mutant showed a significant departure from the *wt* responses (Figs. 2, 3 and S3). On its turn, the loss of function for *rim15* appeared to be dependant on fungus-fungus interactive specificities, as its fungistasis results were statistically distinct between the *R. solani* and *S. sclerotiorum* (Figs. 3 and 4). At last, Skn7 showed to be the least involved in the phenotypic responses, as the results for Δ*skn7* were not different from *wt* for the majority of conditions tested.

When specific volatiles were assessed in the blend emitted by the *T. atroviride* strains (Tables 1 and S1), various interesting aspects could be noticed. First, the total amount and relative proportion of individual VOCs have changed substantially amongst strains. This suggests the loss of function of each RR interfere in the metabolic regulation of volatiles production/emission at some points, although we cannot precisely define where and how this occurs. Moreover, it was possible to observe that with the loss of RRs function, the strains assumed different patterns of VOC emission (Tables 1 and S1), providing further evidence towards a role played by these RRs in the emission and regulation of these compounds in *T. atroviride*. Second, the blend of VOCs in *T. atroviride* tends to be dominated by two compounds, C7–1 and 6PP-1 (Tables 1 and S1), which occurred in highest amounts only in the *wt*. Hence, the data interestingly suggest that Skn7 is likely involved in the synthesis/emission of 6PP1, whereas Ssk1 and Rim15 are likely associated with synthesis/emission of C7–1, because these single compounds sharply decreased their amounts in the blend by the loss of function of those genes in the mutants, respectively (Table 1). Third, the agreement found between the fungistasis activity of *wt* and mutants (Fig. 4) and the corresponding relative amounts of the C7–1, C7–2 and C9–1 compounds in their blends of VOCs (Table 1) suggest these three individual volatiles may specifically have fungistatic action at a distance. When they dropped their presence in the blend, less fungistatic effect was observed (Fig. 4 and Table 1). At this point, we do not know, however, if they are required in a combined manner (amongst themselves and/or with other VOCs) to display the fungistatic activity, and/or if there are some individual or combined thresholds of their amounts to trigger the effect. The fact that C7–1 and C7–2 for Δ*skn7* showed to be in lower absolute amounts than for *wt*, but there was no difference in their fungistatic effects for both pathogens, might suggest the existence of such thresholds. Further experiments controlling the conditions of absolute and relative amounts of these particular VOCs are needed to sort out this issue.

An interesting alternative view for the fungistasis at a distance results when comparing *wt* and mutants is worth noting: since the synthesis/emission of VOCs is also a complex signalling network that allows a fungus to "sense" the presence of other fungi in the environment (Bitas et al., 2013), the loss of function for these RRs might rather be related to such "senseless" phenotype. Under this view, the loss of function for Ssk1 and Rim15 could have reduced the ability of *T. atroviride* in sensing the presence of another fungus (at the *wt* levels), thereby resulting in a decreased (but not eliminated) fungistasis effect. This view is also compatible with the strain/species-specific interactions observed for the *T. atroviride* fungistatic VOCs activities against *R. solani* and *S. sclerotiorum* (Fig. 4), as the ability to sense a given microbe depends on its particular signals emitted, which modulate the VOCs production by *Trichoderma*. Further experiments specifically designed to address this question are certainly warranted.

5. Conclusions

In summary, we showed in this study the potential involvement of three fungal regulators belonging to the two-component regulatory system, namely Skn7, Ssk1 and Rim15, in a variety of cellular responses for stressing/interacting cues in *T. atroviride*, based on single-gene mutation strategy. Taken together, the results suggest that Ssk1 may function as a hub-like RR in *T. atroviride*, as growth, conidiation and interactive phenotypes with plants and other fungi were all affected by the loss of its function. On the other hand, Skn7 did not appear to be critically involved in the majority of those processes, as its functional loss did not significantly alter the mutant phenotype in relation to the *wt*. Finally, the phenotypic results of *Δrim15* to the various stimuli under study seems to confirm the apparent Rim15 participation in modulating cellular responses to nutritional availability (Swinnen et al., 2006), although with a potential cross-talk with other pathways yet to be

defined/confirmed. Although each of the three RRs somehow altered the total production and relative proportion of VOCs, the synthesis/emission of volatiles related to promotion of plant growth was not affected. Moreover, the results combined are suggestive that, for those regulatory processes in which Ssk1 and Rim15 appear to be involved, the former seems to operate upstream to the latter in the corresponding metabolisms. Further investigation addressing specific issues raised by interpretation of our results were indicated, opening new lines of research on two-component response regulators in *Trichoderma* spp.

CrediT author statement

Valter Cruz-Magalhães: Conceptualization, Methodology, Investigation, Original draft preparation, Data curation. **Maria Fernanda Nieto-Jacobo**: Conceptualization, Investigation, Data curation, Methodology. **Michael Rostás**: Conceptualization, Methodology, Validation, Data curation. **Francisco Jesus Echaide-Aquino:** Investigation, Writing- Reviewing and Editing. **Ulises Esquivel Naranjo**: Investigation, Writing- Reviewing and Editing. **Alison Stewart:** Project administration, Funding acquisition. **Artemio Mendoza-Mendoza:** Supervision, Conceptualization, Methodology, Investigation, Data curation, Project administration, Funding acquisition, Writing-Reviewing and Editing; **Leandro Lopes Loguercio**: Supervision, Conceptualization, Project administration, Funding acquisition, Writing- Reviewing and Editing.

Declaration of Competing Interest

The authors do not have conflicts of interest.

Acknowledgments

The authors acknowledge and thank Jason Breitmeyer for his technical assistance with GC–MS analysis, David Saville for his statistical advice and Amanda Soares for the technical assistance in some experiments. This project was supported by the New Zealand Tertiary Education Commission CORE grant to the Bio-Protection Research Centre and Lincoln University Research Fund to A.S. and A.M.-M., and by the Brazilian National Council for Scientific and Technological Development (CNPq) fund (Proc. # 402973/2012–7) to L.L.L. A CNPq fellowship (Proc. SWE # 232182/2014–0) was granted to V.C.-M. for his work at Lincoln University.

Supplementary materials

Supplementary material associated with this article can be found, in the online version, at doi:10.1016/j.crmicr.2022.100139.

References

Adnan, M., Islam, W., Shabbir, A., Khan, K.A., Ghramh, H.A., Huang, Z., Chen, H.Y., Lu, G.D., 2019. Plant defense against fungal pathogens by antagonistic fungi with *Trichoderma* in focus. Microb. Pathog 129, 7–18. https://doi.org/10.1016/j.micpath.2019.01.042.

Bitas, V., Kim, H.S., Bennett, J.W., Kang, S., 2013. Sniffing on microbes: diverse roles of microbial volatile organic compounds in plant health. Mol. Plant Microbe In 26, 835–843. https://doi.org/10.1094/MPMI-10-12-0249-CR.

Brown, J.L., Bussey, H., Stewart, R.C., 1994. Yeast Skn7p functions in a eukaryotic two-component regulatory pathway. EMBO J. 13, 5186–5194. https://doi.org/10.1002/j.1460-2075.1994.tb06849.x.

Casas-Flores, S., Rios-Momberg, M., Bibbins, M., Ponce-Noyola, P., Herrera-Estrella, A., 2004. BLR-1 and BLR-2, key regulatory elements of photoconidiation and mycelial growth in *Trichoderma atroviride*. Microbiology+ 150, 3561–3569. https://doi.org/10.1099/mic.0.27346-0.

Causton, H.C., Ren, B., Koh, S.S., Harbison, C.T., Kanin, E., Jennings, E.G., Lee, T.I., True, H.L., Lander, E.S., Young, R.A., 2001. Remodeling of yeast genome expression in response to environmental changes. Mol. Biol. Cell. 12, 323–337. https://doi.org/10.1091/mbc.12.2.323.

Chauhan, N., Inglis, D., Roman, E., Pla, J., Li, D., Calera, J.A., Calderone, R., 2003. *Candida albicans* response regulator gene SSK1 regulates a subset of genes whose functions are associated with cell wall biosynthesis and adaptation to oxidative stress. Eukaryot. Cell 2, 1018–1024. https://doi.org/10.1128/EC.2.5.1018-1024.2003.

Chen, L.H., Lin, C.H., Chung, K.R., 2012. Roles for SKN7 response regulator in stress resistance, conidiation and virulence in the citrus pathogen *Alternaria alternata*. Fungal Genet. Biol. 49, 802–813. https://doi.org/10.1016/j.fgb.2012.07.006.

Chen, L.H., Tsai, H.C., Yu, P.L., Chung, K.R., 2017. A major facilitator superfamily transporter-mediated resistance to oxidative stress and fungicides requires Yap1, Skn7, and MAP kinases in the citrus fungal pathogen *Alternaria alternata*. PLoS ONE 12, e0169103. https://doi.org/10.1371/journal.pone.0169103.

Cruz-Magalhães, V., Nieto-Jacobo, M.F., van Zijll de Jong, E., Rostás, M., Padilla-Arizmendi, F., Kandula, D., Kandula, J., Hampton, J., Herrera-Estrella, A., Steyaert, J.M., Stewart, A., Lopes Loguercio, L., Mendoza-Mendoza1, A., 2019. The NADPH oxidases Nox1 and Nox2 differentially regulate volatile organic compounds, fungistatic activity, plant growth promotion and nutrient assimilation in *Trichoderma atroviride*. Front. Microbiol. 9, 3271. https://doi.org/10.3389/fmicb.2018.03271.

Cutler, N.S., Pan, X., Heitman, J., Cardenas, M.E., 2001. The TOR signal transduction cascade controls cellular differentiation in response to nutrients. Mol. Biol. Cell 12, 4103–4113. https://doi.org/10.1091/mbc.12.12.4103.

D'Alessandro, M., Erb, M., Ton, J., Brandenburg, A., Karlen, D., Zopfi, J., Turlings, T.C., 2014. Volatiles produced by soil-borne endophytic bacteria increase plant pathogen resistance and affect tritrophic interactions. Plant Cell Environ. 37, 813–826. https://doi.org/10.1111/pce.12220.

De Palma, M., Salzano, M., Villano, C., Aversano, R., Lorito, M., Ruocco, M., Docimo, T., Piccinelli, A.L., D'Agostino, N., Tucci, M., 2019. Transcriptome reprogramming, epigenetic modifications and alternative splicing orchestrate the tomato root response to the beneficial fungus *Trichoderma harzianum*. Hortic. Res. 6, 5. https://doi.org/10.1038/s41438-018-0079-1.

dos Santos, L.B.P.R., Oliveira-Santos, N., Fernandes, J.V., Jaimes-Martinez, J.C., De Souza, J.T., Cruz-Magalhães, V., Loguercio, L.L., 2022. Tolerance to and alleviation of abiotic stresses in plants mediated by *Trichoderma* spp. In: Druzhinina, I.S. (Ed.), Advances in *Trichoderma* Biology and Applications. Chp 15. Springer, New York (*in press*).

Druzhinina, I.S., Seidl-Seiboth, V., Herrera-Estrella, A., Horwitz, B.A., Kenerley, C.M., Monte, E., Mukherjee, P.K., Zeilinger, S., Grigoriev, I.V., Kubicek, C.P., 2011. *Trichoderma*: the genomics of opportunistic success. Nat. Rev. Microbiol. 9, 749–759. https://doi.org/10.1038/nrmicro2637.

El_Komy, M.H., Saleh, A.A., Eranthodi, A., Molan, Y.Y., 2015. Characterization of novel *Trichoderma asperellum* isolates to select effective biocontrol agents against tomato *Fusarium* wilt. Plant Pathol. J. 31, 50. https://doi.org/10.5423/PPJ.OA.09.2014.0087.

Esquivel-Naranjo, E.U., García-Esquivel, M., Medina-Castellanos, E., Correa-Pérez, V.A., Parra-Arriaga, J.L., Landeros-Jaime, F., Herrera-Estrella, A., 2016. A *Trichoderma atroviride* stress-activated MAPK pathway integrates stress and light signals. Mol. Microbiol. 100, 860–876. https://doi.org/10.1111/mmi.13355.

Faria, J.C., Jelihovschi, E.G., Allaman, I.B., 2018. Conventional Tukey Test. UESC, Ilheus, Brasil.

Fassler, J.S., West, A.H., 2011. Fungal Skn7 stress responses and their relationship to virulence. Eukaryot. Cell 10, 156–167. https://doi.org/10.1128/EC.00245-10.

Friedl, M.A., Kubicek, C.P., Druzhinina, I.S., 2008. Carbon source dependence and photostimulation of conidiation in *Hypocrea atroviridis*. Appl. Environ. Microbiol. 74, 245–250. https://doi.org/10.1128/AEM.02068-07.

Hermosa, R., Viterbo, A., Chet, I., Monte, E., 2012. Plant-beneficial effects of *Trichoderma* and of its genes. Microbiology 158, 17–25. https://doi.org/10.1099/mic.0.052274-0.

Hernández-Oñate, M.A., Esquivel-Naranjo, E.U., Mendoza-Mendoza, A., Stewart, A., Herrera-Estrella, A.H., 2012. An injury-response mechanism conserved across kingdoms determines entry of the fungus *Trichoderma atroviride* into development. Proc. Natl. Acad. Sci. U. S. A. 109, 14918–14923. https://doi.org/10.1073/pnas.1209396109.

Hess, J.F., Oosawa, K., Kaplan, N., Simon, M.I., 1988. Phosphorylation of three proteins in the signaling pathway of bacterial chemotaxis. Cell 53, 79–87. https://doi.org/10.1016/0092-8674(88)90489-8.

Hohmann, S., 2002. Osmotic stress signaling and osmoadaptation in yeasts. Microbiol. Mol. Biol. Rev. 66, 300–372. https://doi.org/10.1128/MMBR.66.2.300-372.2002.

Horie, T., Tatebayashi, K., Yamada, R., Saito, H., 2008. Phosphorylated Ssk1 prevents unphosphorylated Ssk1 from activating the Ssk2 mitogen-activated protein kinase kinase kinase in the yeast high-osmolarity glycerol osmoregulatory pathway. Mol. Cell. Biol. 28, 5172–5183. https://doi.org/10.1128/MCB.00589-08.

Hung, R., Lee, S., Bennett, J.W., 2013. Testing the effect of *Trichoderma* volatile organic compounds on *Arabidopsis thaliana*. Phytopathology 103, 63–64.

Inai, T., Watanabe, D., Zhou, Y., Fukada, R., Akao, T., Shima, J., Takagi, H., Shimoi, H., 2013. Rim15p-mediated regulation of sucrose utilization during molasses fermentation using *Saccharomyces cerevisiae* strain PE-2. J. Biosci. Bioeng. 116, 591–594. https://doi.org/10.1016/j.jbiosc.2013.05.015.

Jain, A., Singh, A., Singh, S., Singh, H.B., 2015. Biological management of *Sclerotinia sclerotiorum* in pea using plant growth promoting microbial consortium. J. Basic Microb. 55, 961–972. https://doi.org/10.1002/jobm.201400628.

Jalali, F., Zafari, D., Salari, H., 2017. Volatile organic compounds of some *Trichoderma* spp. increase growth and induce salt tolerance in *Arabidopsis thaliana*. Fungal Ecol. 29, 67–75. https://doi.org/10.1016/j.funeco.2017.06.007.

Ketela, T., Brown, J.L., Stewart, R.C., Bussey, H., 1998. Yeast Skn7p activity is modulated by the Sln1p-Ypd1p osmosensor and contributes to regulation of the HOG pathway. Mol. Gen. Genet. 259, 372–378. https://doi.org/10.1007/s004380050824.

Kottb, M., Gigolashvili, T., Großkinsky, D.K., Piechulla, B., 2015. *Trichoderma* volatiles effecting *Arabidopsis*: from inhibition to protection against phytopathogenic fungi. Front. Microbiol. 6, 995. https://doi.org/10.3389/fmicb.2015.00995.

Leach, M.D., Cowen, L.E., 2014. To sense or die: mechanisms of temperature sensing in fungal pathogens. Curr. Fungal Infect. Rep. 8, 185–191. https://doi.org/10.1007/s12281-014-0182-1.

Lee, S., Hung, R., Yap, M., Bennett, J.W., 2015. Age matters: the effects of volatile organic compounds emitted by *Trichoderma atroviride* on plant growth. Arch. Microbiol. 197, 723–727. https://doi.org/10.1007/s00203-015-1104-5.

Lee, S., Yap, M., Behringer, G., Hung, R., Bennett, J.W., 2016. Volatile organic compounds emitted by *Trichoderma* species mediate plant growth. Fungal Biol. Biotechnol. l, 3. https://doi.org/10.1186/s40694-016-0025-7.

Lee, S., Hung, R., Bennett, J.W., 2014. Interactions between fungi and plants through volatile signaling: the effects of volatile organic compounds (VOCs) emitted by *Trichoderma* on plants. Phytopathology 104, 67. -67.

Li, S., Ault, A., Malone, C.L., Raitt, D., Dean, S., Johnston, L.H., Deschenes, R.J., Fassler, J.S., 1998. The yeast histidine protein kinase, Sln1p, mediates phosphotransfer to two response regulators, Ssk1p and Skn7p. EMBO J. 17, 6952–6962. https://doi.org/10.1093/emboj/17.23.6952.

Liang, S.H., Wu, H., Wang, R.R., Wang, Q., Shu, T., Gao, X.D., 2017. The TORC1–Sch9–Rim15 signaling pathway represses yeast-to-hypha transition in response to glycerol availability in the oleaginous yeast *Yarrowia lipolytica*. Mol. Microbiol. 104, 553–567. https://doi.org/10.1111/mmi.13645.

Liu, J., Wang, Z.K., Sun, H.H., Ying, S.H., Feng, M.G., 2017. Characterization of the Hog1 MAPK pathway in the entomopathogenic fungus *Beauveria bassiana*. Environ. Microbiol. 19, 1808–1821. https://doi.org/10.1111/1462-2920.13671.

Loguercio, L.L., de Carvalho, A.C., Niella, G.R., De Souza, J.T., Pomella, A.W.V., 2009. Selection of *Trichoderma stromaticum* isolates for efficient biological control of witches' broom disease in cacao. Biol. Control 51, 130–139. https://doi.org/10.1016/j.biocontrol.2009.06.005.

Medeiros, H.A.D., Araújo Filho, J.V.D., Freitas, L.G.D., Castillo, P., Rubio, M.B., Hermosa, R., Monte, E., 2017. Tomato progeny inherit resistance to the nematode *Meloidogyne javanica* linked to plant growth induced by the biocontrol fungus *Trichoderma atroviride*. Sci. Rep. 7, 40216. https://doi.org/10.1038/srep40216.

Medina-Castellanos, E., Esquivel-Naranjo, E.U., Heil, M., Herrera-Estrella, A., 2014. Extracellular ATP activates MAPK and ROS signaling during injury response in the fungus *Trichoderma atroviride*. Front. Plant Sci. 5, 659. https://doi.org/10.3389/fpls.2014.00659.

Mirisola, M.G., Taormina, G., Fabrizio, P., Wei, M., Hu, J., Longo, V.D., 2014. Serine-and threonine/valine-dependent activation of PDK and Tor orthologs converge on Sch9 to promote aging. PLoS Genet. 10, e1004113 https://doi.org/10.1371/journal.pgen.1004113.

Mohanta, T.K., Mohanta, N., Parida, P., Panda, S.K., Ponpandian, L.N., Bae, H., 2016. Genome-wide identification of mitogen-activated protein kinase gene family across fungal lineage shows presence of novel and diverse activation loop motifs. PLoS ONE 11, e0149861. https://doi.org/10.1371/journal.pone.0149861. -e0149861.

Montibus, M., Pinson-Gadais, L., Richard-Forget, F., Barreau, C., Ponts, N., 2015. Coupling of transcriptional response to oxidative stress and secondary metabolism regulation in filamentous fungi. Crit. Rev. Microbiol. 41, 295–308. https://doi.org/10.3109/1040841X.2013.829416.

Morgan, B.A., et al., 1997. The Skn7 response regulator controls gene expression in the oxidative stress response of the budding yeast *Saccharomyces cerevisiae*. EMBO J. 16, 1035–1044. https://doi.org/10.1093/emboj/16.5.1035.

Nieto-Jacobo, M.F., Steyaert, J.M., Salazar-Badillo, F.B., Nguyen, D.V., Rostás, M., Braithwaite, M., De Souza, J.T., Jimenez-Bremont, J.F., Ohkura, M., Stewart, A., Mendoza-Mendoza, A., 2017. Environmental growth conditions of *Trichoderma* spp. affects indole acetic acid derivatives, volatile organic compounds, and plant growth promotion. Front. Plant Sci. 8, 102. https://doi.org/10.3389/fpls.2017.00102.

Nodet, P., Capellano, A., Fèvre, M., 1990. Morphogenetic effects of Congo red on hyphal growth and cell wall development of the fungus *Saprolegnia monoica*. Microbiology 136, 303–310. https://doi.org/10.1099/00221287-136-2-303.

Oide, S., Liu, J., Yun, S.H., Wu, D., Michev, A., Choi, M.Y., Horwitz, B.A., Turgeon, B.G., 2010. Histidine kinase two-component response regulator proteins regulate reproductive development, virulence, and stress responses of the fungal cereal pathogens *Cochliobolus heterostrophus* and *Gibberella zeae*. Eukaryot. Cell 9, 1867–1880. https://doi.org/10.1128/EC.00150-10.

Peay, K.G., Kennedy, P.G., Bruns, T.D., 2008. Fungal community ecology: a hybrid beast with a molecular master. Bioscience 58, 799–810. https://doi.org/10.1641/B580907.

Pedruzzi, I., Dubouloz, F., Cameroni, E., Wanke, V., Roosen, J., Winderickx, J., De Virgilio, C., 2003. TOR and PKA signaling pathways converge on the protein kinase Rim15 to control entry into G0. Mol. Cell 12, 1607–1613. https://doi.org/10.1016/S1097-2765(03)00485-4.

Posas, F., Wurgler-Murphy, S.M., Maeda, T., Witten, E.A., Thai, T.C., Saito, H., 1996. Yeast HOG1 MAP kinase cascade is regulated by a multistep phosphorelay mechanism in the SLN1–YPD1–SSK1 "two-component" osmosensor. Cell 86, 865–875. https://doi.org/10.1016/S0092-8674(00)80162-2.

Rodríguez-González, M., Kawasaki, L., Velázquez-Zavala, N., Domínguez-Martín, E., Trejo-Medecigo, A., Martagón, N., Espinoza-Simón, E., Vázquez-Ibarra, A., Ongay-Larios, L., Georgellis, D., de Nadal, E., 2017. Role of the Sln1-phosphorelay pathway in the response to hyperosmotic stress in the yeast *Kluyveromyces lactis*. Mol. Microbiol. 104, 822–836. https://doi.org/10.1111/mmi.13664.

Roncero, C., Duran, A., 1985. Effect of Calcofluor white and Congo red on fungal cell wall morphogenesis: in vivo activation of chitin polymerization. J. Bacteriol. 163, 1180–1185. https://doi.org/10.1128/jb.163.3.1180-1185.1985.

Saito, H., Posas, F., 2012. Response to hyperosmotic stress. Genetics 192, 289–318. https://doi.org/10.1534/genetics.112.140863.

Salas-Marina, M.A., Isordia-Jasso, M.I., Islas-Osuna, M.A., Delgado-Sánchez, P., Jiménez-Bremont, J.F., Rodríguez-Kessler, M., Rosales-Saavedra, M.T., Herrera-Estrella, A., Casas-Flores, S., 2015. The Epl1 and Sm1 proteins from *Trichoderma atroviride* and *Trichoderma virens* differentially modulate systemic disease resistance against different life style pathogens in *Solanum lycopersicum*. Front. Plant Sci. 6, 77. https://doi.org/10.3389/fpls.2015.00077.

Santos, J.L., Shiozaki, K., 2001. Fungal histidine kinases. Sci. STKE 2001 (98), re1. https://doi.org/10.1126/stke.2001.98.re1. PMID: 11752677.

Schmidt, R., Cordovez, V., De Boer, W., Raaijmakers, J., Garbeva, P., 2015. Volatile affairs in microbial interactions. ISME J. 9, 2329–2335. https://doi.org/10.1038/ismej.2015.42.

Schmoll, M., Dattenböck, C., Carreras-Villaseñor, N., Mendoza-Mendoza, A., Tisch, D., Alemán, M.I., Baker, S.E., Brown, C., Cervantes-Badillo, M.G., Cetz-Chel, J., et al., 2016. The genomes of three uneven siblings: footprints of the lifestyles of three *Trichoderma* species. Microbiol. Mol. Biol. Rev. 80, 205–327.

Sorger, P.K., 1991. Heat shock factor and the heat shock response. Cell 65, 363–366. https://doi.org/10.1016/0092-8674(91)90452-5.

Steyaert, J.M., Weld, R.J., Mendoza-Mendoza, A., Stewart, A., 2010. Reproduction without sex: conidiation in the filamentous fungus *Trichoderma*. Microbiology 156, 2887–2900. https://doi.org/10.1099/mic.0.041715-0.

Steyaert, J., Hicks, E., Kandula, J., Kandula, D., Alizadeh, H., Braithwaite, M., Yardley, J., Mendoza-Mendoza, A., Stewart, A., 2016. Methods for the evaluation of the bioactivity and biocontrol potential of species of *Trichoderma*. Microbial-Based Biopesticides. Humana Press, New York, NY, pp. 23–35. https://doi.org/10.1007/978-1-4939-6367-6_3.

Swinnen, E., Wanke, V., Roosen, J., Smets, B., Dubouloz, F., Pedruzzi, I., Winderickx, J., 2006. Rim15 and the crossroads of nutrient signalling pathways in *Saccharomyces cerevisiae*. Cell Div. 1, 1–8. https://doi.org/10.1186/1747-1028-1-3.

Szczałba, M., Kopta, T., Gąstoł, M., Sękara, A., 2019. Comprehensive insight into arbuscular mycorrhizal fungi, *Trichoderma* spp. and plant multilevel interactions with emphasis on biostimulation of horticultural crops. J. Appl. Microbiol. https://doi.org/10.1111/jam.14247.

Team., R.C. 2013. R: a language and environment for statistical computing.

Urban, J., Soulard, A., Huber, A., Lippman, S., Mukhopadhyay, D., Deloche, O., Wanke, V., Anrather, D., Ammerer, G., Riezman, H., Broach, J.R., 2007. Sch9 is a major target of TORC1 in *Saccharomyces cerevisiae*. Mol. Cell 26, 663–674. https://doi.org/10.1016/j.molcel.2007.04.020.

Utkhede, R.S., Sholberg, P.L., 1986. In vitro inhibition of plant-pathogens by *Bacillus subtilis* and *Enterobacter aerogenes* and in vivo control of 2 postharvest cherry diseases. Can. J. Microbiol. 32, 963–967. https://doi.org/10.1139/m86-178.

Waghunde, R.R., Shelake, R.M., Sabalpara, A.N., 2016. *Trichoderma*: a significant fungus for agriculture and environment. Afr. J. Agric. Res. 11, 1952–1965. https://doi.org/10.5897/AJAR2015.10584.

Wang, Z.L., Li, F., Li, C., Feng, M.G., 2014. Bbssk1, a response regulator required for conidiation, multi-stress tolerance, and virulence of *Beauveria bassiana*. Appl. Microbiol. Biotechnol. 98, 5607–5618. https://doi.org/10.1007/s00253-014-5644-4.

Warnes, M.G.R., Bolker, B., Bonebakker, L., Gentleman, R., Huber, W., 2016. Package 'gplots'. Various R programming tools for plotting data. version 3.0. 1. The Comprehensive R Archive Network.

Yu, P.L., Chen, L.H., Chung, K.R., 2016. How the pathogenic fungus *Alternaria alternata* copes with stress via the response regulators SSK1 and SHO1. PLoS ONE 11, e0149153. https://doi.org/10.1371/journal.pone.0149153.

Zeilinger, S., Gupta, V.K., Dahms, T.E., Silva, R.N., Singh, H.B., Upadhyay, R.S., Gomes, E.V., Tsui, C.K.M., Nayak, S.C., 2016. Friends or foes? Emerging insights from fungal interactions with plants. FEMS Microbiol. Rev. 40, 182–207. https://doi.org/10.1093/femsre/fuv045.

Zhang, F., Xu, X., Huo, Y., Xiao, Y., 2019. *Trichoderma*-inoculation and mowing synergistically altered soil available nutrients, rhizosphere chemical compounds and soil microbial community, potentially driving alfalfa growth. Front. Microbiol. 9, 3241. https://doi.org/10.3389/fmicb.2018.03241.